Liquid Crystals
Publication details, including instructions for authors and subscription information:
http://www.informaworld.com/smpp/title~content=t713926090

Controllable alignment of nematics by nanostructured polymeric layers

L. Komitov[a]; G. Barbero [†a]; I. Dahl[a]; B. Helgee[a]; N. Olsson[a]
[a] Liquid Crystal Physics, Department of Physics, Goteborg University, Gothenburg, Sweden

To cite this Article Komitov, L. , Barbero [†], G. , Dahl, I. , Helgee, B. and Olsson, N.(2009) 'Controllable alignment of nematics by nanostructured polymeric layers', Liquid Crystals, 36: 6, 747 — 753
To link to this Article: DOI: 10.1080/02678290902928849
URL: http://dx.doi.org/10.1080/02678290902928849

Liquid Crystals,
Vol. 36, Nos. 6–7, June–July 2009, 747–753

Taylor & Francis
Taylor & Francis Group

INVITED ARTICLE

Controllable alignment of nematics by nanostructured polymeric layers

L. Komitov*, G. Barbero†, I. Dahl, B. Helgee and N. Olsson

Liquid Crystal Physics, Department of Physics, Goteborg University, SE-412 96, Gothenburg, Sweden

(Received 9 February 2009; final form 19 March 2009)

A method for a continuous control of the pretilt angle of the easy axis in the range 0–90° degrees and of the anchoring strength by using nanostructured polymers as alignment layers is described. The nanostructured polymers are blends of two different side-chain polymers each of them promoting planar and homeotropic alignment, respectively. A model to interpret the alignment of a nematic liquid crystal induced by such polymer layers is proposed. We show that in this case the anisotropic part of the surface tension can be approximated by a simple extension of the Rapini–Papoular expression. The predicted trend of the pretilt of the easy axis versus the concentration of the side-chain polymer promoting the planar alignment, for instance, is in good agreement with the experimental data. We also show that the effective anchoring strength of the system depends on the concentration of the side-chain polymer promoting planar alignment, and exhibits a minimum for a well-defined value of this quantity. The results obtained in this work seems to be of importance for liquid crystal displays technology since the control of the pretilt and the anchoring strength strongly affect the performance of liquid crystal displays.

Keywords: titled alignment; anchoring strength; nanostructured polymers; reverse pretilt

1. Introduction

In the absence of external fields, the alignment of liquid crystals in restricted geometries such as sandwich cells is defined by the interactions of the liquid crystal molecules with the surface of the confining solid substrates. The alignment of liquid crystals in displays and devices is of vital importance for the quality of their optical appearance as well as for their performance. Two important parameters are characterizing the alignment of liquid crystals in sandwich cells: (i) the pretilt of the *easy axis*, defining the preferred out-of-substrate plane angle of alignment in the absence of bulk distortions; and (ii) the *anchoring strength*, defined as the curvature of the anisotropic part of the surface energy around the easy axis. These two parameters are highly dependent on the liquid crystal material as well as on the characteristics of the solid surface that the liquid crystal is in contact with (*1*). Some modes of the liquid crystal displays (LCDs) such as twisted nematics and electrically controlled birefringence, for instance, require low pretilt of the easy axis whereas others, such as super twisted nematics and optically compensated birefringence, require high pretilt. Tailoring the easy axis direction and the anchoring strength were and still are the focus of scientists and engineers working in the field of physics and chemistry of LCDs and liquid crystal devices. During the last three decades a lot of work has been done and tremendous progress has been made in this field. Despite the progress, there is still a lack of knowledge about the liquid crystal/solid surface interactions responsible for the alignment of liquid crystals and which have a major impact on their switching properties. Such knowledge, however, is necessary in order to enable the tailoring of the liquid crystal alignment properties so that the best operation conditions for LCDs are provided.

It has been known for quite some time that applying different alignment methods such as evaporation of inorganic materials (e.g. SiOx), using them alone (*2–4*) or in combination with surfactants (*5*), oblique ion bombardment (*6*), etc., enable the achievement of a broad spectrum of pretilt angles. It should be pointed out that none of these methods ensure a reliable continuous control of the pretilt angle or could be considered as appropriate for industrial use. Recently, a method for continuous control of the pretilt has been presented by Yeung *et al.* (*7*). According to this method, a nanostructured alignment layer is used. This alignment layer is prepared from a blend of two standard polyimides promoting vertical and planar alignment, respectively. In the final preparation stage these polyimides are separated into nano-sized domains imposing vertical and planar alignment, respectively. However, the process of nano-segregation of the polyimides is in

*Corresponding author. Email: komitov@physics.gu.se
†Permanent address: Dipartimento di Fisica, Politecnico di Torino, corso Duca degli Abruzzi 24, I-10129 Torino, Italia. Currently a holder of the Marks Guest-Professorship at Gothenburg University.

ISSN 0267-8292 print/ISSN 1366-5855 online

DOI: 10.1080/02678290902928849
http://www.informaworld.com

fact very difficult to control. Yet another method for continuous control of the pretilt from 0° to 90° has been proposed recently by Zhang *et al.* (*8*). According to this method, which is a variant of the method of Yeung *et al*., the alignment film is a sandwich of two alignment layers made of polyimides. The first layer is deposited onto the glass substrate and it has a continuous structure. A second layer is deposited on top of this layer. Since the material of the second layer is not wetting completely the first layer, the second layer has a discontinuous structure with holes. Each of these layers is promoting planar alignment (PA) or vertical alignment (VA), respectively. Consequently, the contact surface of the double alignment layer with the liquid crystal has a heterogenic structure containing areas promoting PA and areas promoting VA, respectively. The pretilt angle, according to this method is controlled by the discontinuity of the second layer, *inter alia* by the concentration of the material of the second layer. However, the dewetting process, much like the phase separation process described above, is a very difficult process to control and reproduce, and some external factors, such as humidity for instance, may strongly affect these processes which, in turn, will affect the amount of pretilt. It should be noted also that the properties of the alignment layers prepared according to these two methods appear to be sensitive with respect to the thickness of the alignment layer (in LCDs with thin-film transistors there is variation of the thickness of the alignment layer due to the surface relief). Therefore, neither the domain separation method nor the double alignment layer method, which moreover is a time-consuming method, are suitable for employment in the LCD industry.

Hence, these two methods enabling continuous control of the pretilt of the easy axis direction are actually difficult to apply in the current LCD technology. The control of the anchoring strength as an important alignment parameter was also a subject of many studies during the last three decades. For instance, in (*9*) it was shown that the anchoring strength of a nematic liquid crystal aligned by a Langmuir–Blodgett monolayer, being a two-component mixture of two fatty acids with different tail lengths, could be effectively controlled by changing the components' ratio. However, even though this is effective, such an alignment method is also not appropriate for the production of LCDs due to its complexity and low degree of reproducibility. The main goal of this work is to suggest and investigate a method enabling the continuous control of both alignment parameters, pretilt angle of the easy axis direction and the anchoring strength, which is appropriate in the production process of LCDs.

2. Experiment

In this work, one-pixel sandwich cells were used. The inner surfaces of the transparent ITO electrodes of the cells were covered with very thin (5–10 nm) alignment layer made from side-chain polymers with mesogenic side-groups. The structure of these polymers is based on our novel alignment HiPAL (high-performance alignment layers) concept (*10*). In this work, two kinds of HiPAL materials were used: with lateral (Figure 1(a)) and with longitudinal (Figure 1(b)) attachment of the mesogenic side-groups to the polymer backbone. HiPAL material with lateral attachment of the side mesogenic groups is promoting PA, whereas HiPAL with longitudinal attachment is promoting VA. Blends containing different ratios of HiPAL-PA and HiPAL-VA materials were prepared. Each of these blends was deposited onto the glass substrates by spin coating of the material from 0.1 wt% solution of the polymer alignment material in tetrahydrofuran. The substrates were first pre-baked at 45°C for 20 min and then baked at 150°C for 45 min. After that they were slowly cooled down to room temperature. The alignment layers were buffed unidirectionally to obtain uniform alignment in the cells. The substrates were assembled in a sandwich cell parallel to each other at distance of about 3μm. The experimental cells were filled under vacuum with the

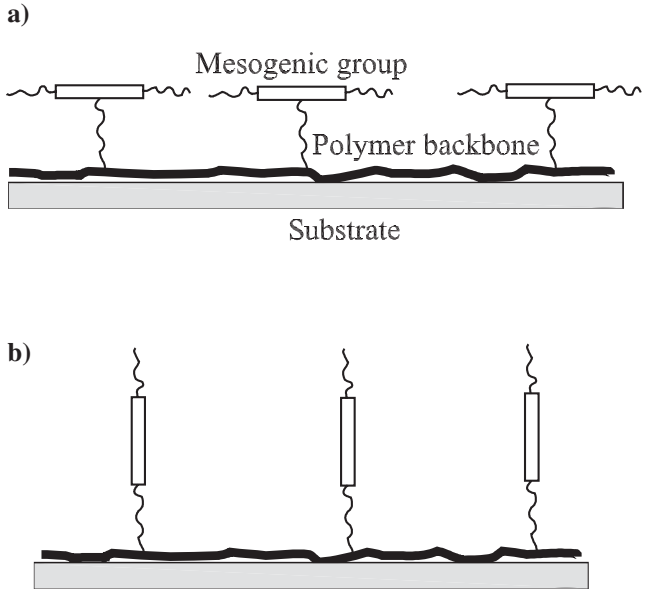

Figure 1. Schematic presentation of the side-chain polymers used in this work as components of the blend for obtaining alignment with a pretilt. The mesogenic groups of these materials are with (a) lateral and (b) longitudinal attachment to the polymer backbone and they are mixed in different proportions in order to obtain different pretilt angles.

liquid crystal materials (both from Merck KGaA, Germany) MLC 6882 ($\Delta\varepsilon < 0$) and MLC 6873-100 ($\Delta\varepsilon > 0$), respectively, in the isotropic phase.

Various methods have been proposed for measuring the pretilt angle of nematic liquid crystal cell substrates. The conoscopic method (*11*), the crystal rotation method (*12*), crystal rotation plus a photoelastic modulator (*13*), the magnetic null method (*14*) and the field-induced birefringence method (*15*) are the most notable. We used a variant of the crystal rotation method, suitable for our thin antiparallel cells (2–3 μm), and suitable also for the whole range of pretilt angles from 0 to 90°. Since we have a Mueller matrix measurement instrument at our disposal (*16*), we were able to measure the retardation with good precision in a small area of the liquid crystal cell. By comparison with numerical simulations, we estimated the pretilt angle.

3. Model

We consider a cell in the shape of a slab of thickness d confined in between two identical surfaces. The director $\mathbf{n}$ is written in terms of the angle θ according to $\mathbf{n} = \cos\theta\mathbf{i} + \sin\theta\mathbf{k}$, where $\mathbf{i}$ and $\mathbf{k}$ are the unit vectors along and perpendicular to the limiting surfaces in the orientation plane, respectively. We assume that the surface energy of nematic liquid crystal in contact with the polymer deposited onto the two confining surfaces is given by (*17*)

$$f = -\frac{1}{2}\left\{w_{\mathrm{H}}\cos^2(\theta-\theta_{\mathrm{H}}) + w_{\mathrm{P}}\cos^2(\theta-\theta_{\mathrm{P}})\right\}, \quad (1)$$

where w_{H} and w_{P} are the anchoring strength due to side groups promoting homeotropic and planar alignment, respectively, and θ_{H} and θ_{P} are the corresponding pretilt angles induced by the rubbing. We suppose that the orienting centres, i.e. the side groups, are uniformly distributed on the surface, with density c_{H} and c_{P}, respectively, where $c_{\mathrm{H}} + c_{\mathrm{P}} = 1$. We indicate this by $c = c_{\mathrm{P}}$ and, hence, $c_{\mathrm{H}} = 1 - c$. Since the anchoring is a result of the interaction of the nematic liquid crystal molecules with the orienting centres attached to the substrates, $w_{\mathrm{H}} = c_{\mathrm{H}}u_{\mathrm{H}} = (1-c)u_{\mathrm{H}}$ and $w_{\mathrm{P}} = c_{\mathrm{P}}u_{\mathrm{P}} = cu_{\mathrm{P}}$, where u_{H} and u_{P} are connected with the interactions responsible for the alignment promoted by the orienting centre. In the absence of external fields, the nematic orientation is constant across the sample, and identical with the easy axis imposed by the surface.

Let us consider first the 'right-angled' case in which $\theta_{\mathrm{H}} = 90°$ and $\theta_{\mathrm{P}} = 0°$. In this case from (1) it follows that the surface energy is given by

$$f = -\frac{1}{2}\left\{w_{\mathrm{H}}\sin^2\theta + w_{\mathrm{P}}\cos^2\theta\right\}. \quad (2)$$

From (2) we obtain

$$\frac{\partial f}{\partial\theta} = \frac{w_{\mathrm{P}} - w_{\mathrm{H}}}{2}\sin(2\theta), \quad (3)$$

$$\frac{\partial^2 f}{\partial\theta^2} = (w_{\mathrm{P}} - w_{\mathrm{H}})\cos(2\theta). \quad (4)$$

The easy direction, θ_e, and the effective anchoring strength, w_e, are defined by

$$\left(\frac{\partial f}{\partial\theta}\right)_{\theta=\theta_e} = 0, \quad w_e = \left(\frac{\partial^2 f}{\partial\theta^2}\right)_{\theta=\theta_e} > 0. \quad (5)$$

In the case under consideration, using (3), the easy axis is defined by $\sin(2\theta_e) = 0$, and hence $\theta_e = 0$ or $\theta_e = 90°$. By taking into account that

$$\left(\frac{\partial^2 f}{\partial\theta^2}\right)_{\theta=0} = w_{\mathrm{P}} - w_{\mathrm{H}}, \quad \text{and} \quad \left(\frac{\partial^2 f}{\partial\theta^2}\right)_{\theta=90°} = w_{\mathrm{H}} - w_{\mathrm{P}}, \quad (6)$$

we conclude that the easy axis is planar ($\theta_e = 0$) for $w_{\mathrm{P}} > w_{\mathrm{H}}$, and homeotropic ($\theta_e = 90°$) for $w_{\mathrm{H}} > w_{\mathrm{P}}$. Since $w_{\mathrm{P}} = cu_{\mathrm{P}}$ and $w_{\mathrm{H}} = (1-c)u_{\mathrm{H}}$, the effective anchoring strength is

$$w_e = |w_{\mathrm{P}} - w_{\mathrm{H}}| = u_{\mathrm{H}}|c(1+u) - 1|, \quad (7)$$

where $u = u_{\mathrm{P}}/u_{\mathrm{H}}$, and it vanishes for $c^* = 1/(1+u)$. For $c < c^*$ the easy axis is homeotropic, whereas for $c > c^*$ it is planar. The transition from the homeotropic to the planar orientation is discontinuous, i.e. it is of first order. The effective anchoring strength depends linearly on c from u_{H} to zero in the region from $c = 0$ to $c = c^*$, and from zero to u_{P} from $c = c^*$ to $c = 1$.

At the transition, the second-order terms vanish completely, and we cannot rule out the possibility that fourth-order terms in the surface energy take over and control the nature of the surface transition. With a $\cos(4\theta)$ term of appropriate amplitude added to (2), we can still obtain a transition from homeotropic to planar. If the added term is independent of c, this transition will be continuous if the term has a positive coefficient and discontinuous if the

coefficient is negative. For a discontinuous transition, there could be coexistence of homeotropic and planar regions, while for a continuous transition there could be competition between pretilt with positive and negative sign. Both of these cases can sometimes be seen in experimental cells.

Let us consider now the general case $\theta_H \neq 90^\circ$ and $\theta_P \neq 0^\circ$, where f is given by (1). Such values of θ_H and θ_P are the simplest way to incorporate the symmetry-breaking effect of unidirectional rubbing in the theory. Routine calculations give

$$\frac{\partial f}{\partial \theta} = \frac{1}{2}\{w_H \sin[2(\theta - \theta_H)] + w_P \sin[2(\theta - \theta_P)]\}, \quad (8)$$

$$\frac{\partial^2 f}{\partial \theta^2} = w_H \cos[2(\theta - \theta_H)] + w_P \cos[2(\theta - \theta_P)]. \quad (9)$$

From (5), we obtain that the easy axis is defined by

$$\tan(2\theta_e) = \frac{w_H \sin(2\theta_H) + w_P \sin(2\theta_P)}{w_H \cos(2\theta_H) + w_P \cos(2\theta_P)}, \quad (10)$$

and the anchoring strength by

$$w_e = \sqrt{w_H^2 + 2w_H w_P \cos[2(\theta_H - \theta_P)] + w_P^2}. \quad (11)$$

From (10) and (11) it follows that when $\theta_H = 90^\circ$ and $\theta_P = 0$, $\tan(2\theta_e) = 0$, and $w_e = |w_P - w_H|$, in agreement with the results reported above. We observe that $w_P/w_H = u[c/(1-c)]$, where u has been defined after (7). Consequently, θ_e and w_e depend on c.

Equation (10) has to be inverted by taking into account that for $c = 0$, $\theta_e = \theta_H$, and for $c = 1$, $\theta_e = \theta_P$. Simple calculations give

$$\theta_e = \arccos\sqrt{\frac{w_H \cos(2\theta_H) + w_e + w_P \cos(2\theta_P)}{2w_e}}, \quad (12)$$

where w_e is given by (11). In Figure 2, we show the dependence of θ_e versus c for two values of u, when $\theta_H = 85^\circ$ and $\theta_P = 10^\circ$, whereas in Figure 3 we show the same dependence for two values of θ_H with $\theta_P = 0$ and $u = 1$. Note that as $\theta_H \to 90^\circ$ and $\theta_P \to 0^\circ$ the dependence of θ_e versus c tends to that described in the first part of the paper. In Figure 4, we show the dependence of $\theta_e = \theta_e(c)$ for two different values of the pretilt θ_p.

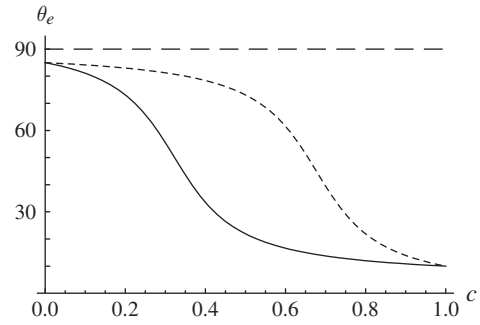

Figure 2. Plot of θ_e versus c for $\theta_H = 85^\circ$ and $\theta_P = 10^\circ$. Solid curve $u = 2$, dotted curve $u = 0.5$. The the dashed line indicates the 90° level.

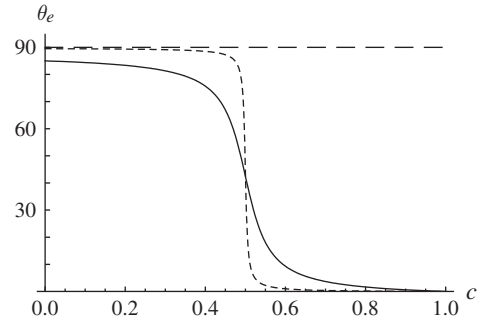

Figure 3. Plot of θ_e versus c for $u = 1$ and $\theta_P = 0$. Solid curve $\theta_H = 85^\circ$, dotted curve $\theta_H = 89.5^\circ$.

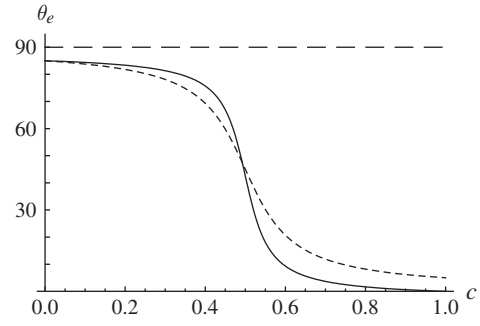

Figure 4. Plot of θ_e versus c for $u = 1$ and $\theta_H = 85^\circ$. Solid curve $\theta_p = 0^\circ$, dotted curve $\theta_P = 5^\circ$.

From (12) simple calculations show that

$$\frac{\partial \theta_e}{\partial c} < 0, \quad \text{for all } c, \quad (13)$$

$$\frac{\partial^2 \theta_e}{\partial c^2} = 0, \quad \text{for } c^* = \frac{1 - u\cos[2(\theta_H - \theta_P)]}{1 + u^2 - 2u\cos[2(\theta_H - \theta_P)]}. \quad (14)$$

From (13) it follows that θ_e is a decreasing function of c. From (14) we deduce that for $c = c^*$, $|\partial\theta_e/\partial c|$

reaches its maximum value. If we consider also $\partial^2\theta_e/\partial c^2$, it is possible to show that it reaches its extrema in

$$c_{1,2} = \frac{3 - 3u(3+u^2)\cos[2(\theta_H - \theta_P)] + 3u^2\{2 + \cos[4(\theta_H - \theta_P)]\}}{3\{1 + u^2 - 2u\cos^2[2(\theta_H - \theta_P)]\}} \mp \frac{u\sqrt{3\{1 + u^2 - (u/2)\sin^2[4(\theta_H - \theta_P)]\}}}{3\{1 + u^2 - 2u\cos^2[2(\theta_H - \theta_P)]\}}. \quad (15)$$

The quantities $c_{1,2}$ define the borders of the region where θ_e depends on c in a quasi-linear manner.

Let us consider now the dependence of w_e on c. From (11), considering that $w_H = (1-c)u_H$ and $w_P = cu_P$, we have

$$w_e = u_H\sqrt{\{1 + u^2 - 2u\cos[2(\theta_H - \theta_P)]\}c^2} + \sqrt{2\{u\cos[2(\theta_H - \theta_P)] - 1\}c + 1}, \quad (16)$$

from which it follows that

$$\frac{\partial w_e}{\partial c} = u_H\frac{\{1 + u^2 - 2u\cos[2(\theta_H - \theta_P)]\}c + u\cos[2(\theta_H - \theta_P)] - 1}{\sqrt{\{1 + u^2 - 2u\cos[2(\theta_H - \theta_P)]\}c^2 + 2\{u\cos[2(\theta_H - \theta_P)] - 1\}c + 1}}. \quad (17)$$

Equation (17) shows that w_e reaches its minimum value for $c = c^*$ given by (14). The value of $w_e = w_e(c^*)$ is

$$w_e(c^*) = u_H\frac{u\sin[2(\theta_H - \theta_P)]}{\sqrt{1 + u^2 - 2u\cos[2(\theta_H - \theta_P)]}}. \quad (18)$$

We note that for $\theta_H = 90^\circ$ and $\theta_P = 0^\circ$, according to (14), $c^* = 1/(1+u)$ and from (18), $w_e(c^*) = 0$, in agreement with the results reported in the first part of the paper. In Figure 5 we show $w_e = w_e(c)$. As discussed above, w_e presents a well-defined minimum for $c = c^*$, whose value is given by (18). Near this minimum the potential might become shallow if $\theta_H - \theta_P$ is near 90° and then there is a chance for fourth-order terms to influence the behaviour. If we also in this case add a cos(4θ) term, we could obtain a flat potential or a discontinuous jump in the θ_e value, if the term is added with negative coefficient, and a possible metastable state with reversed tilt if the coefficient is positive, see Figure 6. Similar observations were made by Wang *et al.* (*18*). Neither is usually wanted, so a balance should be sought. Both of these cases can sometimes be seen in experimental cells, and the second case is illustrated in Figure 7.

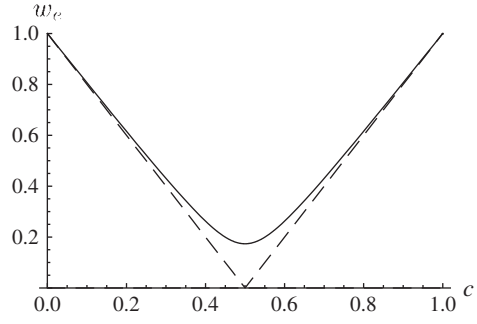

Figure 5. Plot of w_e versus c for $u = 1$ and $\theta_H = 85^\circ$, $\theta_P = 5^\circ$. The dashed line illustrates the surface energy with zero pretilt.

In Figure 8, we show the experimentally obtained pretilt angles for the liquid crystals MLC-6882 (negative dielectric anisotropy) and MLC-6873-100 (positive dielectric anisotropy), using as alignment layers the polymer blends described in the experimental part, and compare them with the best fit obtained by means of (12).

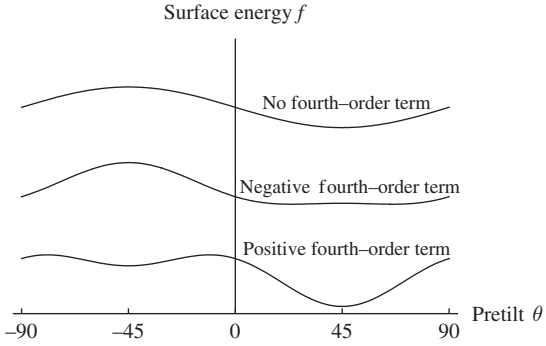

Figure 6. Comparison of the surface potential for three cases for small positive pretilt angles θ_H and θ_P. Without the fourth-order term the pretilt has one minimum position. With the negative fourth-order cos(4θ) term, the minimum is flatter, and might be split into two adjacent minima. With the positive fourth-order term the minimum is deeper, but we also obtain another local minimum with reversed pretilt angle.

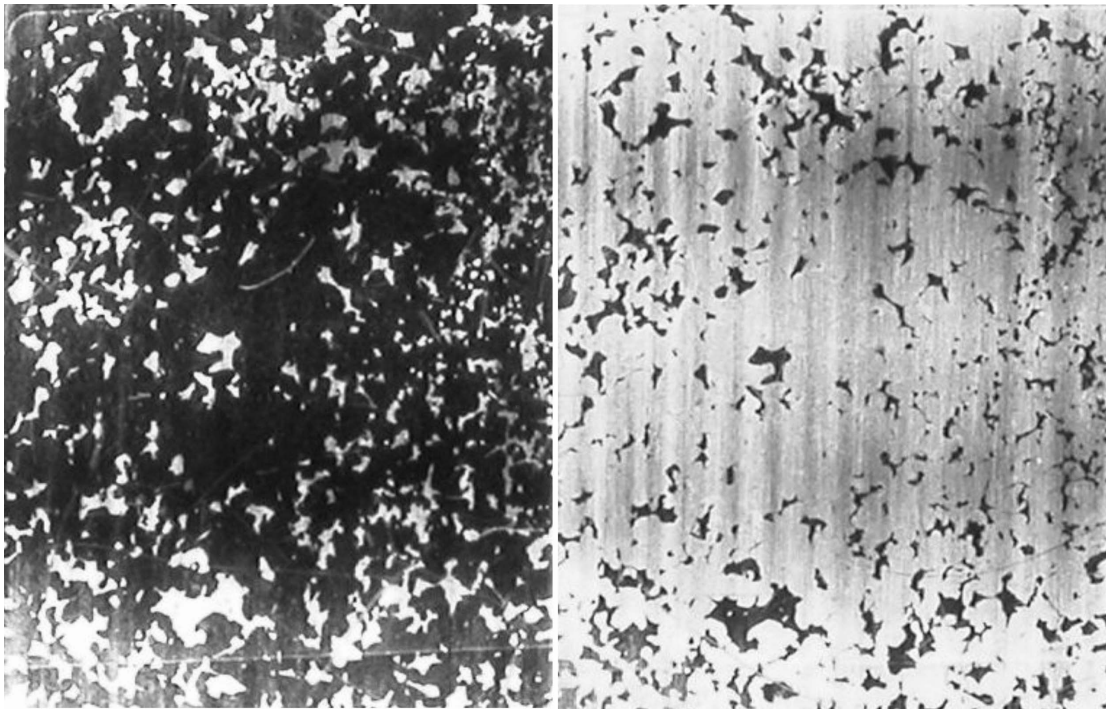

Figure 7. The central part of a nematic cell. We look oblique along the molecules in most of the cell in the left picture, but see some areas where the tilt is reversed ('flakes'). If we look at the cell from the other side, the contrast is reversed. We can also see that the orientation is sensitive to the rubbing conditions.

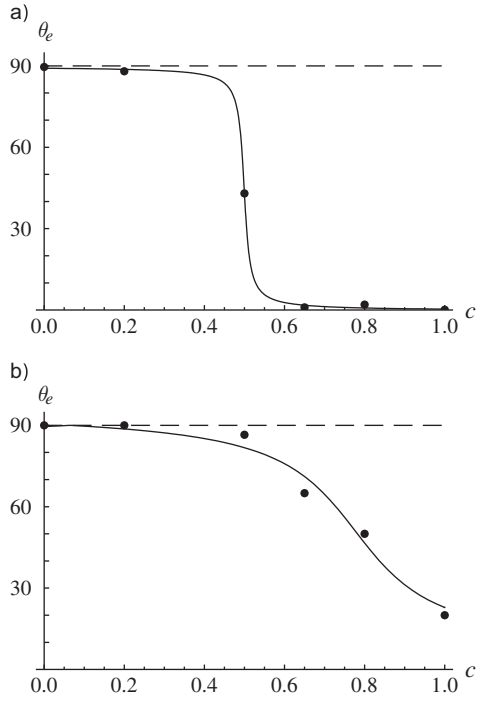

Figure 8. Best fit of the experimental data (points), with the theoretical expression for θ_e given by (12) (continuous curve). The best fit for the liquid crystal MLC-6882 is obtained for $u = 1.00$ and $\theta_H = 89.1°$, $\theta_P = 0.35°$. For MLC-6873-100 the best fit is obtained for $u = 0.34$, $\theta_H = 90.5°$ rad, and $\theta_P = 22.8°$.

For MLC-6882 the best fit is obtained for $u = 1.00$, $\theta_H = 89.1°$, and $\theta_P = 0.35°$. For MLC-6873-100 the best fit is obtained for $u = 0.34$, $\theta_H = 90.5°$, and $\theta_P = 22.8°$. The agreement between the best fit and the experimental data is rather good for all c.

4. Summary

In this work we have presented a method for continuous control of the pretilt angle of the easy axis direction. According to this method, nanostructured alignment materials enable continuous control of the pretilt from 0 to 90°. These materials are blends of two HiPAL materials, promoting planar and homeotropic alignment. The magnitude of the pretilt depends on the ratio of the components in the blends. In contrast to the method reported in (*7*) and (*8*), the nanostructured alignment layers used in our work possess a continuous structure, i.e. the miscibility of the components is very good and no separation occurs. In a certain range of concentrations the pretilt exhibits a linear dependence on the concentration. To explain the mechanisms behind the alignment properties of the nanostructured alignment materials we proposed a theoretical model in which a homogeneous distribution of the orienting centres is assumed, i.e. of the side groups of the polymeric material.

We have shown that the anisotropic part of the surface tension of a nematic liquid crystal limited by a solid substrate covered by a nanostructured polymer can be obtained by means of a simple extension of the Rapini–Papoular expression. According to our analysis the surface easy axis and the effective anchoring strength depend on the concentration of the orienting centres. The agreement between the experimental data and the theoretical model is rather good on the full range of the investigated concentration of planar orienting centres. Hence, we can deduce that the hypothesis on which is based our model are sufficiently close to reality. In particular:

(1) the orienting centres are uniformly distributed;
(2) the orienting forces are of short range;
(3) the surface energy for planar and homeotropic alignment are proportional to the densities of the relevant orienting centres.

From our model it follows that the effective anchoring strength exhibits a well-defined minimum for a given concentration of the surface orienting centres. This allows us to control the anchoring strength as well, and thus to control the switching characteristics of LCDs, such as the threshold voltage, V_{th}, and rise τ_r and fall τ_f times of the cell, since they are highly dependent on the anchoring strength (*10*).

Acknowledgement

GB is grateful to the University of Gothenburg for awarding him the position of Marks Guest-Professorship.

References

(1) Priezjev, N.V.; Skacej, G.; Pelcovits, R.A.; Zumer, S. *Phys. Rev. E* **2003**, *68*, 041709-1–041709-6.
(2) Janning, J.L. *Appl. Phys. Lett.* **1972**, *21*, 173–174.
(3) Monkade, M.; Boix, M.; Durand, G. *Europhys. Lett.* **1988**, *5*, 697–702.
(4) Jerome, B.; Pieranski, P.; Boix, M. *Europhys. Lett.* **1988**, *5*, 693–696.
(5) Hauck, G.; Komitov, L.; Derzhanski, A.; Koswig, H.D. *Cryst. Res. Technol.* **1982**, *17*, 865–869.
(6) Chaudhari, P.; Lacey, J.; Doyle, J.; Galligan, E.; Alan Lien, S.-C.; Callegari, A.; Hougham, G.; Lang, N.D.; Andry, P.S.; John, R.; Yang, K.-H.; Lu, M.; Cai, C.; Speidell, J.; Purushothaman, S.; Ritsko, J.; Samant, M.; Stohr, J.; Nakagawa, Y.; Katoh, Y.; Saitoh, Y.; Sakai, K.; Satoh, H.; Odahara, S.; Nakano, H.; Nakagaki, J.; Shiota, Y. *Nature* **2001**, *411*, 56–59.
(7) Yeung, F.S.; Ho, J.Y.; Li, Y.W.; Xie, F.C.; Tsui, O.K.; Sheng, P.; Kwok, H.S. *Appl. Phys. Lett.* **2006**, *88*, 051910-1–051910-3. Kwok, H.S.; Yeung, F.S. *J. SID* **2008**, *16*, 911–918.
(8) Zhang, K.; Liu, N.; Twieg, R.; Auman, B.; Bos, P. *Liq. Cryst.* **2008**, *35*, 1191–1197.
(9) Fazio, V.S.U.; Nannelli, F.; Komitov, L. *Phys. Rev. E* **2001**, *63*, 061712-1–061712-8.
(10) Komitov, L. *Thin Solid Films* **2008**, *516*, 2639–2644.
(11) Komitov, L.; Hauck, G.; Koswig, H.D. *Cryst. Res. Technol.* **1984**, *19*, 253–260.
(12) Baur, G.; Wittwer, V.; Berreman, D.W. *Phys. Lett. A* **1975**, *56*, 142–142.
(13) Li, Y.W.; Yeung, F.S.Y.; Tan, L.; Ho, J.Y.L.; Kwok, H.S. *The 13th International Display Workshops (IDW'06)*, December, pp. 223–226.
(14) Scheffer, T.J.; Nehring, J. *J. Appl. Phys.* **1977**, *48*, 1783–92.
(15) Hsu, J.S.; Liang, B.-J.; Chen, S.-H. *IEEE Trans. Electron. Devices* **2005**, *52*, 918–921.
(16) Dahl, I. *Meas. Sci. Technol.* **2001**, *12*, 1938–1948.
(17) Rapini, A.; Papoular, M. *J. Phys. Colloq. (France)* **1969**, *30*, 54–58.
(18) Wang, R.; Atherton, T.J.; Zhu, M.; Petschek, R.G.; Rosenblatt, C. *Phys. Rev. E* **2007**, *76*, 021702-1–021702-5.